Eur. Phys. J. A **40**, 127–130 (2009)
DOI 10.1140/epja/i2009-10756-y

THE EUROPEAN PHYSICAL JOURNAL A

Letter

Letter

Assignment of levels in ^{208}Fr and 10^- isomers in the odd-odd isotones ^{206}At and ^{208}Fr

G.D. Dracoulis[1,a], P.M. Davidson[1], G.J. Lane[1], A.P. Byrne[1,2], T. Kibédi[1], P. Nieminen[1,3], A.N. Wilson[1,2], and H.Watanabe[1,4]

[1] Department of Nuclear Physics, R.S. Phys. S.E, Australian National University, Canberra ACT 0200, Australia
[2] Department of Physics, Australian National University, Canberra ACT 0200, Australia
[3] Department of Physics, University of Jyväskylä, P.O. Box 35, (YFL) FIN-40014, Finland
[4] Nuclear Physics Research Division, RIKEN Nishina Center, 2-1 Hirosawa, Wako, Saitama, 351-0198, Japan

Received: 12 January 2009 / Revised: 1 March 2009
Published online: 22 March 2009 –
Communicated by N. Alamanos

Abstract. Excited states in ^{208}Fr have been identified using the ^{197}Au(^{16}O, 5n)^{208}Fr reaction and a variety of time-correlated γ-ray and conversion electron spectroscopic techniques. Transitions above and below a $\tau = 623(16)$ ns 10^- isomer are placed in the level scheme. This isomer is analogous to that observed in the odd-odd isotone ^{206}At for which additional spectroscopic information is also obtained, including a precise lifetime of $\tau = 1173(30)$ ns. The γ-rays assigned to ^{208}Fr are the same as the main transitions erroneously assigned to ^{209}Fr in previous work.

PACS. 21.10.Tg Lifetimes, widths – 23.20.Lv γ transitions and level energies – 23.35.+g Isomer decay – 27.80.+w $190 \leq A \leq 219$

Nuclei above the $Z = 82$ closed proton shell and below the $N = 126$ closed neutron shell provide an important region for testing shell model structures, defining residual interactions and probing possible transitions to non-spherical shapes. The francium isotopes ($Z = 87$) are known in some detail from the closed neutron shell at $N = 126$ down to the $N = 124$ isotope ^{211}Fr [1,2]. Information on the lighter isotopes, however, is more limited. A number of excited states in ^{210}Fr have been assigned from the α-decay of ^{214}Ac [3] although these are necessarily of relatively low spin. A recent study by a Yale group reported a set of transitions for ^{210}Fr and a partial level scheme for ^{209}Fr [4]. However, our work, aimed initially at defining the structure of ^{209}Fr, does not agree with those assignments [5]. Rather, the transitions assigned to ^{209}Fr in ref. [4] are in fact from ^{208}Fr, while the γ-rays that had been assigned to ^{210}Fr belong in ^{209}Fr. The new assignments are based in part on excitation functions for (^{16,17,18}O, xn) reactions on ^{197}Au and will be covered in detail elsewhere (ref. [5]). Note, however, that the measurements with ^{18}O beams lead via 4n evaporation to the well-established case of ^{211}Fr, thus providing an indirect calibration of the oxygen-induced reaction. Note also that our assignment is in fact consistent with pre-existing cross-section measurements for the (^{16}O, xn) reactions (see, for example, refs. [6–9]). Some information on the still lighter range of isotopes, $^{205-207}$Fr, has also recently been reported [10].

Although the main coincidence measurements were carried out with ^{16}O ions on ^{197}Au at an energy of 95 MeV with a 5 mg/cm^2 thick target in order to optimize the 4n evaporation channel leading to ^{209}Fr, 5n evaporation leading to ^{208}Fr was significant. A level scheme for ^{208}Fr has thus been established and is the main subject of this report. The structures observed are similar to those identified in the isotone ^{206}At [11] which is also populated in the present study through the ^{197}Au(^{16}O, α3n)^{206}At reaction, allowing both confirmation of its scheme and additional information of relevance to be obtained, specifically, a precise value for the lifetime of the 10^- isomer.

The measurements were carried out in conjunction with studies of the spectroscopy of ^{212}Rn [12], using similar measurement and analysis techniques. To populate the francium nuclei, pulsed beams of oxygen isotopes were provided by the ANU, 14UD Pelletron accelerator. Pulses of about 1 ns in width, separated by 1716 ns were used in the main γ-γ-time measurements, which were complemented by γ-time measurements with a beam of nanosecond pulses separated by 19 μs. The CAESAR array comprised six Compton-suppressed hyperpure Ge detectors,

[a] e-mail: George.Dracoulis@anu.edu.au

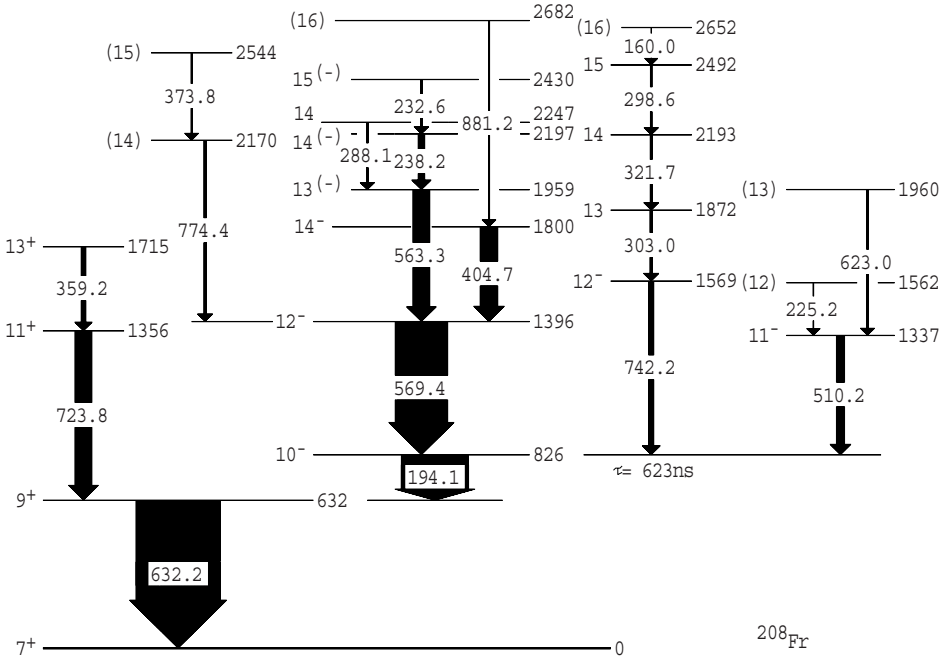

Fig. 1. Level scheme of ^{208}Fr deduced from the present work.

three larger volume Ge detectors (also Compton suppressed and 80% efficient) and two LEPS detectors. The first six Compton-suppressed detectors are arranged in pairs in the vertical plane, at angles with respect to the beam direction of $\pm 97°$, $\pm 148°$ and $\pm 48°$, allowing γ-ray anisotropies to be measured.

Gamma-gamma-time matrices were constructed from these data to establish the coincidence relationships. Additional time conditions were used to select γ-rays feeding or following isomers. Lifetime information was obtained by projecting intermediate-time spectra from γ-γ-time cubes with gates on γ-rays above and below the state of interest, as well as from the γ-ray-time data with respect to the nanosecond-pulsed and chopped beams.

Angular-anisotropy information to constrain multipolarities was obtained from both the singles γ-ray measurements and also from the γ-γ coincidence data constrained to select transitions above specific isomeric states. The latter was accomplished by constructing three matrices of transitions observed in any of the three pairs of six detectors in the vertical plane (defining three angles with respect to the beam axis), on one axis, with either prompt or delayed transitions observed in the other eight large detectors. Gates were set to isolate specific transitions assigned to the scheme, without contamination. Spectra were constructed from which three-point anisotropies could be determined, with appropriate corrections for the angle and energy-dependent relative efficiencies.

Some conversion coefficients were measured directly using a superconducting solenoid to transport electrons to a cooled Si(Li) detector, with simultaneous measurement of γ-rays in a single Compton-suppressed detector in the arrangement described in ref. [13]. Gamma-rays and electrons were measured with respect to a pulsed beam of ^{16}O, with pulses separated by 6.5 μs, conditions chosen to allow the subtraction of activities and other contaminants from the transitions associated with isomers in ^{209}Fr and ^{208}Fr, by appropriate time-gating. A target with a thickness of 2.4 mg/cm^2 was used with its plane at 30° to the beam axis, as a compromise between the maintenance of electron resolution (electrons being observed through the back of the target and at 90° to the beam axis) and the need to stop most of the recoiling nuclei.

The level scheme deduced for ^{208}Fr is shown in fig. 1. The only significant lifetime observed was that assigned to the 826 keV state, which decays by a 194 keV transition to a 632 keV state that is assumed to decay to the known 7^+ ground state. A total conversion coefficient of $\alpha_T \leq 0.16$ (2σ level) was obtained for the 194 keV transition from delayed intensity balances, defining it as of $E1$ multipolarity, while for the 632 keV transition, the electron measurements gave $\alpha_K = 0.014(2)$, to be compared with a theoretical $E2$ value of $\alpha_K(E2) = 0.0155$. Together with the anisotropies and the absence of other lifetimes or branches, this information leads to the assignment of 9^+ for the 632 keV state and 10^- for the 826 keV state. This agrees with the recent isotopic assignment for 194 and 632 keV γ-rays obtained (with Z and A identification) in the fragmentation reaction study by Podolyak *et al.* [14]. They associated these γ-rays with the decay of an isomer in ^{208}Fr, with $T_{1/2} \sim 200$ ns, analogous to the 10^- isomer in ^{206}At.

The main transitions placed in the level scheme can be seen in the γ-ray spectra given in fig. 2. Intensities and anisotropies are listed in table 1. The most intense transition above the 10^- isomer is the 569 keV γ-ray through which the main cascade proceeds. Figure 2(a) shows the spectrum of lines in prompt coincidence with it, while fig. 2(b) was obtained with time constraints that select γ-rays that precede the delayed 194 and 632 keV transi-

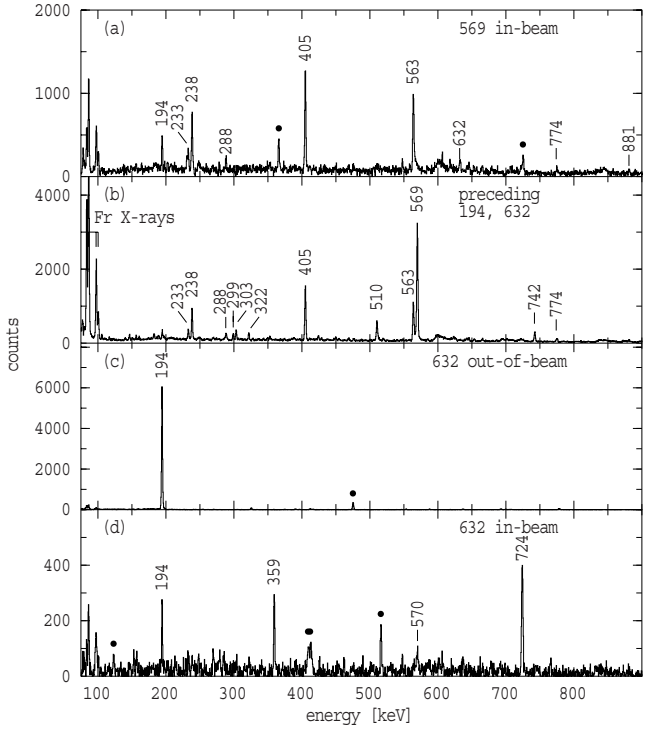

Fig. 2. Selected γ-ray spectra with various γ-ray energy and time constraints: a) transitions in prompt coincidence with the 569 keV transition that feeds the 10^- isomer, b) transitions that precede the 194 keV and 632 keV cascade below the isomer, c) prompt coincidences in the out-of-beam time region with a gate on the 632 keV γ-ray and d) prompt coincidences in a $\pm$ 40 ns region around the beam pulse, with a gate on the 632 keV γ-ray. Contaminants are marked by filled circles.

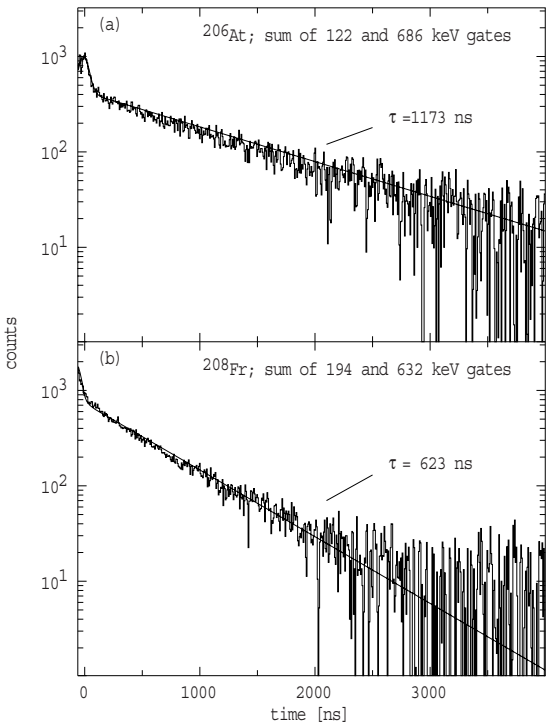

Fig. 3. Representative time spectra obtained with a chopped beam for transitions below the 10^- isomer in a) ^{206}At and b) ^{208}Fr. Note that the final lifetimes were deduced from a combination of fits to these spectra (solid lines) and to equivalent spectra from other pulsed beam measurements.

Table 1. Transitions assigned to ^{208}Fr.

E_γ	I_γ	$A_2/A_0{}^{(a)}$	E_i	E_f	J_i^π	J_f^π
160.0	5(1)		2652	2492	17	16
194.1	799(14)		826	632	10^-	9^+
225.2	10(3)		1562	1337	(12)	11^-
232.6	25(2)	−0.62(15)	2430	2197	$15^{(-)}$	$14^{(-)}$
238.2	80(4)	−0.67(9)	2197	1959	$14^{(-)}$	$13^{(-)}$
288.1	22(2)	−0.41(19)	2247	1959	14	$13^{(-)}$
298.6	21(2)	−0.17(24)	2492	2193	15	14
303.0	33(2)	−0.14(19)	1872	1569	13	12^-
321.7	27(2)	−0.27(18)	2193	1872	14	13
359.2	57(5)	+0.29(11)	1715	1356	13^+	11^+
373.8	15(3)		2544	2170	(15)	(14)
404.7	213(8)	+0.37(11)	1800	1396	14^-	12^-
510.2	99(6)	−0.50(13)	1337	826	$11^{(-)}$	10^-
563.3	202(7)	−0.42(7)	1959	1396	$13^{(-)}$	12^-
569.4	624(14)	+0.35(6)	1396	826	12^-	10^-
623.0	19(4)		1960	1337	(13)	11
632.2	1000	+0.21(5)	632	0	9^+	7^+
723.8	203(10)	+0.28(8)	1356	632	11^+	9^+
742.2	65(5)	+0.29(19)	1569	826	12^-	10^-
774.4	31(4)	+0.08(22)	2170	1396	(14)	12^-
881.2	15(4)		2682	1800	(16)	14^-

(^{a}) Three-point anisotropy fitted to a second-order Legendre polynomial.

tions. The γ-rays that bypass the isomer (except for the remnant 194 keV transition) and directly feed the 632 keV state can be seen in fig. 2(d). Note that the intensity of the higher-lying transitions drops rapidly, a consequence mainly of the relatively low beam energy compared to the optimum energy for the reaction, but also partly because of the competition with fission which depletes the higher l-values in the reaction.

There are essentially three separate cascade paths above the isomer, proceeding through the 569, 742 and 510 keV γ-rays. These γ-rays have anisotropies consistent with the stretched quadrupole character for the first two, and dipole for the third. In the absence of any significant lifetimes, quadrupole transitions are assumed to be $E2$ in character, while dipoles could be $E1$, $M1$ or, for large anisotropies, mixed $M1/E2$, leading to suggested assignments of 12^- for both the 1396 and 1569 keV states, and 11^- for the 1337 keV state. Similar considerations lead to the spins and parities given in fig. 1 and table 1.

In the case of ^{206}At, the 10^- isomer decays via a 122 keV $E1$ transition to a 686 keV 9^+ state [11], giving a 122/686 keV cascade equivalent to the 194/632 keV cascade assigned here to ^{208}Fr. Figure 3 shows representative time spectra obtained with the chopped beam for both cascades from one of our measurements. There were several independent sources for determining the lifetimes in our work including direct timing with respect to pulsed and chopped beams with several pulse separations (1.7 μs, 6 μs and 19 μs) and the intermediate times from the γ-γ-

Table 2. Transition strengths for $E1$ decays from the 10^- isomers in ^{206}At and ^{208}Fr.

E_γ	α_T [15]	$B(E\lambda)$ (e^2 fm^2)	Transition strength (W.u.)
		^{206}At: 1173(30) ns	
121.6	0.285	$2.32(6)\times10^{-7}$	$1.03(3)\times10^{-7}$
		^{208}Fr: 623(16) ns	
194.1	0.0947	$1.26(3)\times10^{-7}$	$5.56(14)\times10^{-8}$

time data covering a ±850 ns range. These lead to adopted values of $\tau = 623(16)$ ns for ^{208} Fr and $\tau = 1173(30)$ ns for the isomer in ^{206}At. The latter value, which corresponds to $T_{1/2} = 813(21)$ ns, is a factor of two higher than the value of $T_{1/2} = 410(80)$ ns reported in ref. [11], a discrepancy which can probably be attributed to the restricted time range of ±300 ns used in those measurements.

The corresponding $E1$ transition strengths are summarized in table 2. These are comparable to each other (although not identical) and in the region of 10^{-7} W.u., typical of hindered $E1$ transitions in the lead region (see, for example, ref. [16]).

Some of the hindrance can be attributed to the configuration change between the initial and final states. The 10^- state is from the $\pi[h^n_{9/2}]_{9/2} \otimes \nu i^{-1}_{13/2}$ configuration (proton seniority-one; $n = 3$ for At and $n = 5$ for Fr) while the 9^+ state will be from the seniority-three proton configuration coupled to the $f_{5/2}$ neutron hole. The 7^+ ground state involves the same proton configuration with seniority-one coupled to the $f_{5/2}$ neutron hole. Although the maximum spin in the first case would give an 11^- state, this is unfavored by the repulsive proton-particle, neutron-hole interaction for parallel coupling [17]. The relevant two-particle interactions are $\langle \pi h_{9/2} | \nu i^{-1}_{13/2} \rangle_{11^-} = +886$ keV, and $\langle \pi h_{9/2} | \nu i^{-1}_{13/2} \rangle_{10^-} = +30$ keV [18]. The 11^- state observed at 1337 keV, 510 keV above the 10^- isomer is an obvious candidate for the unfavored aligned state. The (proton) seniority-three $\pi[h^5_{9/2}] \otimes \nu f^{-1}_{5/2}$ configuration will also give rise to states with $J^\pi = 11^+$ and 13^+, identified with the experimental states at 1356 and 1715 keV. In considering the other states feeding the 10^- isomer, it should be noted that not all have firmly assigned parities. Nevertheless, mostly negative-parity states are expected at low energies from coupling of the $f_{5/2}$ neutron hole (and other neutron-hole pairs) to the seniority-three and seniority-five $h^4_{9/2} i_{13/2}$ proton configuration or from the $i_{13/2}$ neutron hole coupled to the $h^5_{9/2}$ or $h^4_{9/2} f_{7/2}$ proton configuration.

Finally, the excitation energy of the 10^- configuration in the range of francium and astatine isotopes is directly related to the energy of the $i_{13/2}$ neutron-hole excitation in the odd-Pb isotopes. While the proton excitations are relatively constant, the $13/2^+$ neutron-hole state drops rapidly and is known at 425, 629, 825 and 1014 keV in the isotopes ^{199}Pb, ^{201}Pb, ^{203}Pb and ^{205}Pb respectively. The other factor that controls the properties of the 10^- state is the energy of the 9^+ proton excitation which changes relatively slowly as a function of the neutron number. With inclusion of the additional residual interactions, the net result is that in ^{206}Fr, the (10^-) state identified at 531 keV above the 7^+ state (presumably) falls below the 9^+ excitation, so that only an inhibited $E3$ decay is possible, resulting in a half-life of 0.7 s [19,20]. On similar grounds a 10^- excitation could be expected in ^{210}Fr at about 800 keV above the 7^+ state, probably with a somewhat higher energy $E1$ decay to a 9^+ state than is the case in ^{208}Fr, leading to a shorter-lived isomer. Future studies of both ^{208}Fr at optimized beam energies and ^{210}Fr, addressing both this and other aspects of the nuclear structure are anticipated.

The authors are grateful to the staff of the ANU Heavy Ion Accelerator Facility for their continuing support.

References

1. A.P. Byrne, G.D. Dracoulis, C. Fahlander, H. Hübel, A.R. Poletti, A.E. Stuchbery, J. Gerl, R.F. Davie, S.J. Poletti, Nucl. Phys. A **448**, 137 (1986).
2. A.P. Byrne, R. Müsseler, H. Hübel, M. Murzel, K. Theine, W. Schmitz, K.H. Maier, H. Kluge, H. Grawe, H. Haas, Phys. Lett. B **217**, 38 (1989).
3. P. Kuusiniemi, F.P. Heßberger, D. Ackermann, S. Hofmann, I. Kojouharov, Eur. Phys. J. A **22**, 429 (2004).
4. D.A. Meyer *et al.*, Phys. Rev. C **73**, 024307 (2006).
5. G.D. Dracoulis, P.M. Davidson, G.J. Lane, A.P. Byrne, T. Kibédi, P. Nieminen, H. Watanabe, A.N. Wilson, submitted to Phys. Rev. C.
6. S. Baba *et al.*, Z. Phys. A **331**, 53 (1988).
7. G. Stancari *et al.*, Nucl. Instrum. Methods A **557**, 390 (2006).
8. L. Corradi *et al.*, Phys. Rev. C **71**, 014609 (2005).
9. K.-T. Brinkmann, A.L. Caraley, B.J. Fineman, N. Gan, J. Velkovska, R.L. McGrath, Phys. Rev. C **50**, 309 (1994).
10. D.J. Hartley *et al.*, Phys. Rev. C **78**, 054319 (2008).
11. X.C. Feng *et al.*, Eur. Phys. J. A **6**, 235 (1999).
12. G.D. Dracoulis, G.J. Lane, A.P. Byrne, P.M. Davidson, T. Kibédi, P. Nieminen, H. Watanabe, A.N. Wilson, Phys. Lett. B **662**, 19 (2008).
13. T. Kibédi, G.D. Dracoulis, A.P. Byrne, Nucl. Instrum. Methods Phys. Res. A **294**, 523 (1990).
14. Zs. Podolyák *et al.*, *Proceedings of Frontiers in Nuclear Structure Astrophysics and Reactions, FINUSTAR*, AIP Conf. Proc. **831**, 114 (2006).
15. T. Kibédi, T.W. Burrows, M.B. Trzhaskovskaya, P.M. Davidson, C.J. Nestor jr., Nucl. Instrum. Methods A **589**, 202 (2008).
16. T. Lönnroth, Z. Phys. A **331**, 11 (1988).
17. J.P. Schiffer, W.W. True, Rev. Mod. Phys. **48**, 191 (1976).
18. S. Bayer, A.P. Byrne, G.D. Dracoulis, A.M. Baxter, T. Kibèdi, F.G. Kondev, S.M. Mullins, T.R. McGoram, Nucl. Phys. A **650**, 3 (1999).
19. B.G. Ritchie, K.S. Toth, H.K. Carter, R.L. Mlekodaj, E.H. Spejewski, Phys. Rev. C **23**, 2342 (1981).
20. M. Huyse, P. Decrock, P. Dendooven, G. Reusen, P. Van Duppen, J. Wauters, Phys. Rev. C **46**, 1209 (1992).